

Wet surface and dense atmosphere on early Mars suggested by the bomb sag at Home Plate, Mars

Michael Manga,¹ Ameeta Patel,¹ Josef Dufek,² and Edwin S. Kite¹

Received 28 October 2011; revised 29 November 2011; accepted 30 November 2011; published 5 January 2012.

[1] We use the Mars Exploration Rover Spirit observation of a bomb sag produced by an explosive volcanic eruption to infer the atmospheric density at the time of eruption. We performed analogue experiments to determine the relationship between the wetness of the substrate and the velocity and density of impacting clasts and 1) the formation (or not) of bomb sags, 2) the morphology of the impact crater, and 3) the penetration depth of the clast. The downward deflection of beds seen on Mars is consistent with water-saturated sediment in the laboratory experiments. Collision angles <20 degrees from vertical are needed to produce bomb sags. From the experiments we infer an impact velocity up to 4×10^1 m/s, lower than ejection velocities during phreatic and phreatomagmatic eruptions on Earth. If this velocity represents the terminal subaerial impact velocity, atmospheric density exceeded 0.4 kg/m^3 at the time of eruption, much higher than at present. **Citation:** Manga, M., A. Patel, J. Dufek, and E. S. Kite (2012), Wet surface and dense atmosphere on early Mars suggested by the bomb sag at Home Plate, Mars, *Geophys. Res. Lett.*, 39, L01202, doi:10.1029/2011GL050192.

1. Introduction

[2] The evolution of the Martian atmosphere is one of the most engaging questions in planetary science. While much work has focused on the plausibility of an early, dense atmosphere, the total atmospheric pressure of early Mars remains poorly constrained (reviewed by *Jakosky and Phillips* [2001]). Total atmospheric pressure, and the partial pressure of water, have likely played a role in shaping the morphology of almost all surface features on the planet. Most notably, climate and the phase stability of liquid water at the surface of the planet are tied to atmospheric pressure [e.g., *Richardson and Mishna*, 2005]. In addition, near surface vesiculation of magmas, geochemical weathering environments on the surface, aeolian transport of particles, and the potential habitability of the planet, are all influenced by atmospheric pressure.

[3] Small scale, explosive volcanic eruptions can be approximated as point sources that loft material of many different sizes into the atmosphere, and thus offer an opportunity to probe atmospheric density indirectly by examining the sorting of these particles and structures in their deposits. The observations by the Mars Exploration Rover Spirit of the

Home Plate deposits offer compelling evidence that they have an explosive volcanic origin [*Squyres et al.*, 2007]. The structure, stratigraphy and bed forms resemble those of maars, though a source vent has not been identified [*Lewis et al.*, 2008]. Maars are circular volcanic structures, typically a few hundred meters to a few kilometers in diameter, formed by phreatic and phreatomagmatic eruptions [e.g., *Lorenz*, 1973]. Ballistically deposited rock fragments that create bomb sags are characteristic of maar deposits [e.g., *Schmincke*, 2004] and, indeed, a bomb sag was identified at Home Plate (Figure 1a) [*Squyres et al.*, 2007]. Phreatomagmatic eruptions occur when ascending batches of magma rapidly heat and vaporize reservoirs of either liquid water or ice in the shallow sub-surface. Vaporization creates a high-pressure lens of gas that fragments the surrounding country-rock, sends larger blocks on ballistic trajectories, and entrains juvenile magmatic particles and country rock into particle-laden gravity currents. The intensity of the initial blast, the trajectory and momentum of ballistic particles, and the dynamics of the gravity current are all influenced by atmospheric density [e.g., *Fagents and Wilson*, 1996; *Wilson and Head*, 2007].

[4] Here we use attributes of the bomb sag in Figure 1a to estimate atmospheric density at the time of eruption and the saturation state of the substrate onto which the rock fragment fell. We use laboratory experiments to identify controls on the main features of bomb sags. As impact sags are generally taken as evidence that “deposits were moist to wet” [*Lorenz*, 2007] we first document the effect of water on the morphology of impact sags. Next we obtain a relationship between the depth of particle penetration, particle size, and impact velocity, from which we can infer atmospheric density from the observed bomb sag.

2. Experimental Methods

[5] To create laboratory bomb sags, we propelled cm-sized particles with compressed air towards a bed of sand-sized particles. The impacting particles were either 1.3 cm diameter glass spheres (density 2.4 g/cm^3), natural scoria particles (mean long, intermediate and short lengths of 13.0, 9.3, and 7.3 mm, respectively, and density 1.0 g/cm^3), or 1.3 cm diameter stainless steel balls (density 7.7 g/cm^3). The stainless steel balls are used to test scaling relationships. The experimental bed was made by pouring 30 mesh sand (0.60 ± 0.17 mm major axis, 0.43 ± 0.12 mm minor axis) into a $30 \times 30 \times 30$ cm box. This volume is large enough that neither the sides [*Goldman and Umbanhowar*, 2008] nor the bottom [*Sequin et al.*, 2008] influence penetration. There was no additional consolidation. The sand bed was recreated every few experiments. In experiments designed to study the deformation of the substrate, we created layered

¹Department of Earth and Planetary Science and Center for Integrative Planetary Science, University of California, Berkeley, California, USA.

²Earth and Atmospheric Sciences, Georgia Institute of Technology, Atlanta, Georgia, USA.

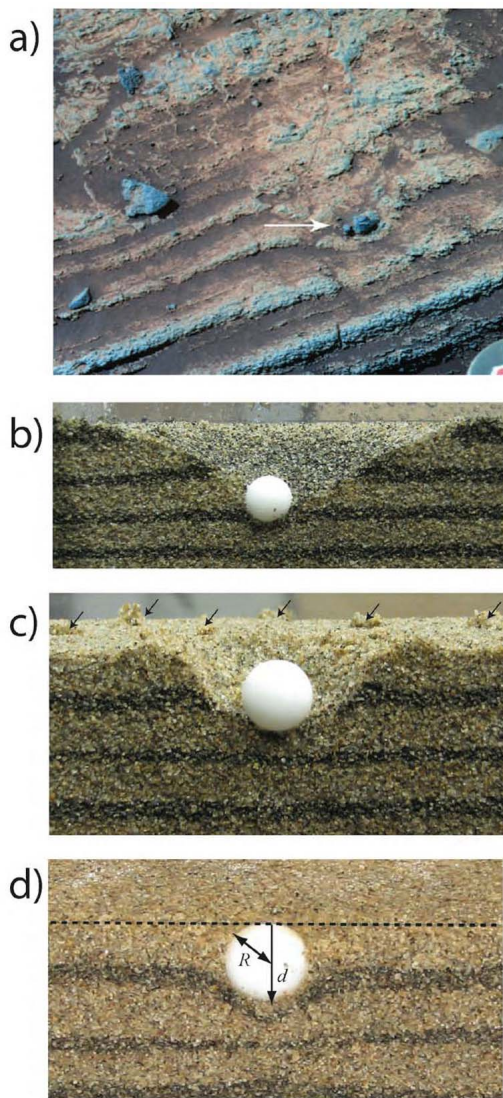


Figure 1. (a) Bomb sag identified by Mars Exploration Rover Spirit, Home Plate, Mars. Clast is 3.8 cm wide [Lewis *et al.*, 2008]. Vertical slice through the bomb sag experiments with glass spheres for (b) dry sand, (c) damp sand (arrows indicate clots of ejected damp sand), and (d) water saturated sand. In Figure 1d, the horizontal dashed line indicates the sand surface, d is the penetration depth, and $2R$ in the particle diameter. The layering was horizontal prior to each experiment, and layering is defined by different color sand grains. Vertical slices were made after saturating the sand and then allowing gravity to drain excess water – this provides cohesion to the sand. Velocities are 47.4, 45.7, and 43.7 m/s, for Figures 1b, 1c, and 1d, respectively. High resolution jpeg at http://www.nasa.gov/images/content/175701main_mer20070503hisres-c.jpg.

substrates with alternating layers of dark and light colored sand with otherwise similar properties.

[6] Our choice of sand size is based on the size of particles in the Home Plate beds. The Microscopic Imager on the rover measured 0.2–0.4 mm diameter particles in the “upper unit” that overlie the “lower unit” in which the bomb sag was found [Squyres *et al.*, 2007]. The lower unit does not at present have a clastic texture, either because the grain size is

smaller than the resolution of the imager (0.1 mm), or more likely because diagenesis has obscured the original texture [Lewis *et al.*, 2008]. Knobby structures in the lower unit have diameters of ~ 1 mm [Lewis *et al.*, 2008]. These structures in the lower unit have been interpreted as accretionary lapilli [Wilson and Head, 2007].

[7] We considered dry sand, water saturated sand, and damp sand in which the sand was saturated and then allowed to drain under the influence of gravity. The Home Plate observations agree best with morphologies produced in water-saturated sand (section 3) and we thus performed most of our experiments with water-saturated substrates.

[8] We varied impact velocity from 3–54 m/s for the glass beads, 3–89 m/s for the scoria particles, and 3–32 m/s for the stainless steel balls. These velocities are close to, but also somewhat less than, typical ejection velocities of ballistic clasts at maars and phreatic eruptions on Earth, 50–120 m/s [e.g., Self *et al.*, 1980; Le Guern *et al.*, 1980; Mastin, 1991; Fagents and Wilson, 1993; Valentine *et al.*, 2011; Sottili *et al.*, 2011]. Maximum velocities and clast sizes are limited by safety concerns. Velocity was measured using a high-speed camera that recorded 1000 frames per second. Collision angle ϕ , measured with respect to vertical, was varied from 0 to 40 degrees.

3. Qualitative Observations: Bomb Sag Morphology

[9] Figure 1 shows substrate deformation produced for different saturation conditions. The impacting particles are the same, 13 mm diameter glass spheres with velocities of ~ 44 m/s. In dry sand, layers are deflected upward in the vicinity of the particle, and sand particles are ejected from the crater created by the impact. In damp sand, clots of damp sand are ejected from the crater and the layered structure is undisturbed. Ejected clumps of sand are visible in Figure 1c. In water-saturated sand, the layers are deflected downward by the impacting particle and comparatively less sand is ejected from the crater. Penetration depth is greatest in dry sand, and smallest in water-saturated sand.

4. Quantitative Observations: Bouncing Particles and Penetration Depth

[10] Figure 2 shows the fraction of particles that create bomb sags as a function of impact angle ϕ for 10–16 experiments at each angle. We define a bomb sag as a crater that retains the particle. For angles $> 20^\circ$, particles are not retained in the crater created by the impact. For reasons we do not understand, low density scoria is less likely to be retained in their craters.

[11] The inset of Figure 2 shows the velocity of the glass spheres and whether they are retained within the crater (filled triangles), or bounce out of it (open circles). The mean velocity of particles that formed bomb sags, 28 ± 15 m/s, is essentially identical to those that did not, 32 ± 16 m/s implying that impact velocity does not affect whether particles remain in the craters they form. This is also the case for dry materials [e.g., Nishida *et al.*, 2010].

[12] Figure 3a shows penetration depth d normalized by particle diameter $2R$ as a function of impact velocity. We use the vertical component of velocity U as previous experiments found that work done scales with the velocity normal

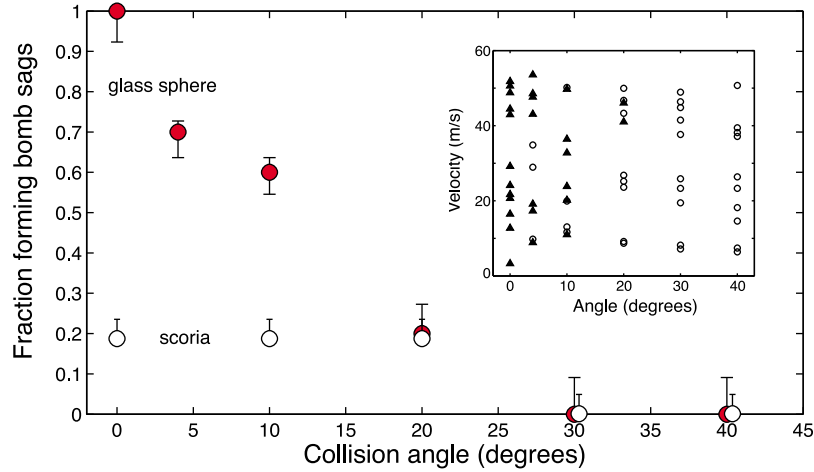


Figure 2. Fraction of sag-forming impacts in water-saturated sand as a function of collision angle (measured with respect to vertical) for glass spheres (filled circles) and natural scoria (open circles). Inset shows details of the glass sphere experiments and the velocity of the impacts that formed bomb sags (filled triangles) and those that did not (open circles).

to the surface [Sklar and Dietrich, 2004]. We show only measurements for water-saturated sand. For a given velocity, more dense particles have a greater penetration depth.

[13] The penetration of objects into granular materials is of widespread interest and the subject of many studies, in part because it probes granular mechanics. The most closely related experiments to those we present here are impacts into dry granular materials, at speeds low enough that particles are not buried, in which

$$\frac{d}{2R} = c \left[\left(\frac{\rho_p}{\rho_s \mu^2} \right)^{3/2} \frac{U^2}{2gR} \right]^{1/3} \quad (1)$$

for a wide range of all parameters, except gravity g which could not be varied (modified from Uehara *et al.* [2003] according to Katsuragi and Durian [2007]). Here ρ_p and ρ_s are particle and substrate density, respectively, μ is the tangent of the angle of repose, and c is a dimensionless scaling constant. For our experiments we use measured $\rho_s = 2.1 \text{ g/cm}^3$ and a repose angle of 35° . The expression on the right hand side is a dimensionless impact energy, which scales with U^2 , though the normalization is empirical and lacks a theoretical derivation [Newhall and Durian, 2003]. We assume the same functional form applies to our wet sand experiments. Figure 3b shows that the normalization in equation (1) collapses our data to a single curve, at least over the limited range of parameters we are able to investigate. A best fit to all the data gives $c = 0.0234 \pm 0.0006$; if we assume the exponent $1/3$ is a free parameter, a best-fit gives $c = 0.022 \pm 0.008$ and an exponent of 0.0340 ± 0.008 , consistent with equation (1).

[14] The scatter in the measurements is larger than the uncertainties of the measurements. This is similar to other measurements of impact-related properties of natural volcanic materials including energy loss upon collision [Cagnoli and Manga, 2003; Dufek and Manga, 2008], or whether particles bounce [Dufek *et al.*, 2009]. Scatter in the present experiments likely reflects the heterogeneity of bed properties including variations in the force chain networks [e.g., Liu *et al.*, 1995; Daniels *et al.*, 2004] and small variations in

particle concentration and hence particle packing [e.g., Royer *et al.*, 2011; de Bruyn and Walsh, 2004]. We are not able to create identical beds at the grain-by-grain scale for the experiments, nor do we expect that surge deposits and other natural substrates will have spatially homogeneous granular structures. We thus suggest that the scatter in Figure 3 identifies the uncertainties and limitations to

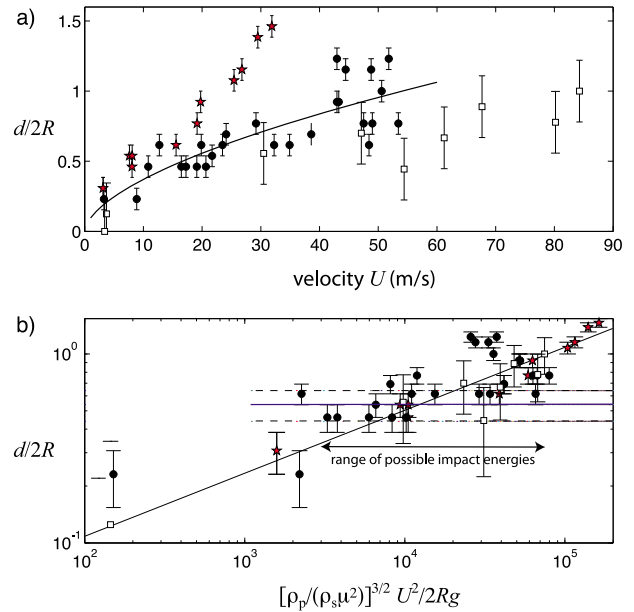


Figure 3. (a) Dimensionless penetration depth (depth d divided by particle diameter $2R$) as a function of impact velocity (stars: stainless steel; open squares: scoria; filled circles: glass). Curve is best fit to the glass sphere data, $d/2R = 0.096U^{0.588}$. (b) Same data as in Figure 3a but impact velocity is normalized as proposed by Newhall and Durian [2003]; curve is best fit to equation (1) with $c = 0.0233$. The Home Plate bomb sag has $d/2R = 0.54 \pm 0.1$, indicated by the horizontal black and dotted lines. Values on the abscissa between 3×10^3 and 6×10^4 are consistent with the observed penetration depth.

quantitative analysis of the penetration depth of natural bomb sags.

5. Discussion

[15] Our experiments allow us to assess the role of substrate saturation, impact angle, and impact velocity on the formation of bomb sags. We now attempt to use the laboratory experiments to provide constraints on the substrate and atmospheric density at the time of the Home Plate eruption.

[16] We begin by emphasizing some of the limitations that must be kept in mind as we interpret the experiments. Foremost, Spirit imaged only one bomb sag, so we have a limited ability to assess uncertainty. We thus focus on the ability to reject the hypothesis that atmospheric density was similar to that at present. Additional caveats: we have not considered the effect of grain shape, size distribution and sorting in the substrate; our laboratory bombs are smaller than the one at Home Plate; we are unable to measure the three-dimensional shape of the bomb and impact crater; the experiments were not performed in a reduced gravity environment.

[17] The Home Plate bomb sag (Figure 1a) most closely resembles the water-saturated morphology in Figure 1d. We thus infer that the lower unit at Home Plate was also wet at the time of eruption. Water saturated conditions may imply a warmer temperature due to a warmer climate, melting of snow or ground ice by hot pyroclastic material, or a warmer subsurface produced by hydrothermal activity maintained by the volcanic system that created the eruption [e.g., *Schmidt et al.*, 2008]. Localized water saturation can also be achieved during phreatic eruptions when the initial steam blast expands and cools, and liquid water coats particles or aggregates of ash [e.g., *Latham et al.*, 2011]. We do not favor deposition over actively degassing sediments as no degassing features are evident, and the layering in Figure 1a is well defined and preserved.

[18] There are other blocks in Figure 1a that do not have sags. This could indicate changing substrate conditions or the blocks could be impact ejecta, but we suggest that this may reflect the small probability of forming sags, as shown in Figure 2. The Home Plate sag is likely not proximal to the vent owing to the small number of blocks and well-sorted deposits [*Lewis et al.*, 2008] so large collision angles are possible.

[19] *Lewis et al.* [2008] made topographic measurements to ensure that the apparent bed deflection seen in Figure 1a is not a consequence of viewing geometry or outcrop orientation. Based on their stereo data there is a 1.4 cm deflection, d' , in the vertical direction. Assuming normal impact to the bed (Figure 2), and bed slopes δ between 10° and 30° (K. Lewis personal communication, 2011), the penetration depth $d = d'/\cos\delta$ is between 1.4 and 1.6 cm. For bomb size, we use the mean of the long and short axes, 3.8 cm and 1.8 cm based on the work of *Lewis et al.* [2008], to estimate $2R = 2.8$ cm. The penetration depth $d/2R$ is thus 0.54 ± 0.1 . Our experimental measurements in Figure 3 thus imply values on the abscissa between 3×10^3 and 6×10^4 .

[20] To obtain an impact velocity we assume a clast density of 2.4 g/cm^3 , because the bomb size suggests that it is a lithic fragment and not a juvenile clast [*Wilson and Head*, 2007]. From equation (1), the implied impact velocity is

thus between 10 m/s and 40 m/s. This is similar to the range of 10 to 50 m/s we would infer from Figure 3a, assuming that the lab experiments apply directly, and unscaled, to Mars. The ranges we report are based on the range of experimental data rather than being obtained from best-fit equations.

[21] Impact velocities are lower than typical ejection velocities at maars on Earth (section 2). Ejection velocities should be comparable on both planets. Bombs and other granular material ejected during the eruption are initially accelerated by the pressure difference between steam and the weight of overlying material. Atmospheric pressure, on Earth or Mars, is a small contribution compared to lithostatic and critical point pressures, and the initial acceleration is likely insensitive to atmospheric conditions. Only later do atmospheric drag and gravity substantially influence the trajectory and velocity of the clasts.

[22] We consider the possibility that the low impact velocity was caused by atmospheric drag. We assume impact at the terminal velocity

$$u_{\text{term}} = \sqrt{\frac{2mg}{\rho A C_d}} \quad (2)$$

where m is clast mass, g is gravity, ρ atmosphere density, A particle cross-section area, and C_d is the drag coefficient. We use a clast diameter of 2.8 cm. C_d is between 0.1 and 0.5 [*Achenbach*, 1972]. This range of drag coefficients is appropriate for particle Reynolds numbers between 10^3 – 10^7 which should encompass gas properties for atmospheres with pressures from 10^2 – 10^6 Pa. The laminated bedding suggests dilute density currents, so we can neglect enhanced drag from particle-particle collisions [*Dufek et al.*, 2009]. A terminal velocity of <40 m/s implies minimum atmospheric densities of 0.4 kg/m^3 ; for comparison, the present atmosphere density on Mars is 0.02 kg/m^3 and the density of Earth's atmosphere at STP is 1.3 kg/m^3 . Despite uncertainties in the terms used to evaluate (2), the inferred density is clearly larger than at present.

[23] The implications for the nature and evolution of early Mars climate are attended by a few important caveats. First, the observation probes an unknown point in time. Orbital imagery of Gusev crater shows that Home Plate lies on areally restricted Noachian inliers [*Rice et al.*, 2010] rather than the extensive early Hesperian ~ 3.65 Ga Gusev lava plains [*Greeley et al.*, 2005]. However, the Home Plate deposits themselves may be Hesperian or younger. Second, we assume the clast was ejected by a hydromagmatic eruption and that ejection velocities are comparable to those on Earth, and attribute the low impact velocity to atmospheric drag (though we cannot exclude the possibility that the sag may have been produced by a particle that bounced and hence had lower velocity). We do not favor purely ballistic transport at velocities less than the terminal velocity because a collision angle $<20^\circ$ (Figure 2) and impact velocity <40 m/s (Figure 3), require a proximal vent within 350 m, and the Home Plate deposits do not appear to be proximal [*Lewis et al.*, 2008]. There are, however, two mounds, “Goddard” and “von Braun”, that are ~ 200 m away [*Rice et al.*, 2010] that could be sources. Third, deposition into standing water would lower the impact velocity on the substrate. Fourth, the inference of a wet surface does not require a much

warmer climate. A density $>10 \text{ kg/m}^3$ is required for a $\text{CO}_2\text{-H}_2\text{O}$ greenhouse to main annually-averaged surface temperatures above freezing [Haberle, 1998]; such a high density is not favored by the penetration depth implying i) the water reflects seasonal and local melting, ii) melting is due to volcanic processes, or iii) other greenhouse gases were responsible for warm temperatures.

6. Conclusions

[24] Bomb sag morphology favors impact onto a water-saturated surface. The observed penetration depth is consistent with subaerial impact velocities lower than 40 m/s, lower than typical ejection velocities in hydromagmatic eruptions on Earth. An atmosphere density higher than at present is thus suggested by the Home Plate observations, though any inferences are limited by having only one observation of a bomb sag. Similar observations elsewhere will help test and extend our inferences, as would constraints on the source vent location.

[25] **Acknowledgments.** We thank K. Lewis and reviewers for their insights and suggestions. Supported by NASA grant NNX09AL20G.

[26] The Editor thanks Kevin Lewis and Ralph Lorenz for their assistance in evaluating this paper.

References

- Achenbach, E. (1972), Experiments on flow past spheres at very high Reynolds numbers, *J. Fluid Mech.*, *54*, 565–575, doi:10.1017/S0022112072000874.
- Cagnoli, B., and M. Manga (2003), Pumice-pumice collisions and the effect of impact angle, *Geophys. Res. Lett.*, *30*(12) 1636, doi:10.1029/2003GL017421.
- Daniels, K. E., J. E. Coppock, and R. P. Behringer (2004), Dynamics of meteor impacts, *Chaos*, *14*, S4, doi:10.1063/1.1821711.
- de Bruyn, J. R., and A. M. Walsh (2004), Penetration of spheres into loose granular media, *Can. J. Phys.*, *82*, 439–446, doi:10.1139/p04-025.
- Dufek, J., and M. Manga (2008), In situ generation of ash in pyroclastic flows, *J. Geophys. Res.*, *113*, B09207, doi:10.1029/2007JB005555.
- Dufek, J., J. Wexler, and M. Manga (2009), The transport capacity of pyroclastic density currents: Experiments and models of substrate-flow interaction, *J. Geophys. Res.*, *114*, B11203, doi:10.1029/2008JB006216.
- Fagents, S. A., and L. Wilson (1993), Explosive volcanic eruptions-VII. The ranges of pyroclasts ejected in transient volcanic explosions, *Geophys. J. Int.*, *113*, 359–370, doi:10.1111/j.1365-246X.1993.tb00892.x.
- Fagents, S., and L. Wilson (1996), Numerical modeling of ejecta dispersal from transient volcanic explosions on Mars, *Icarus*, *123*, 284–295, doi:10.1006/icar.1996.0158.
- Goldman, D. I., and P. Umbanhowar (2008), Scaling and dynamics of sphere and disk impact into granular media, *Phys. Rev. E*, *77*, 021308, doi:10.1103/PhysRevE.77.021308.
- Greeley, R., B. H. Foing, H. Y. McSween Jr., G. Neukum, P. Pinet, M. van Kan, S. C. Werner, D. A. Williams, and T. E. Zegers (2005), Fluid lava flows in Gusev crater, Mars, *J. Geophys. Res.*, *110*, E05008, doi:10.1029/2005JE002401.
- Haberle, R. M. (1998), Early Mars climate models, *J. Geophys. Res.*, *103*, 28,467–28,479, doi:10.1029/98JE01396.
- Jakosky, B. M., and R. J. Phillips (2001), Mars' volatile and climate history, *Nature*, *412*, 237–244, doi:10.1038/35084184.
- Katsuragi, H., and D. J. Durian (2007), Unified force law for granular impact cratering, *Nat. Phys.*, *3*, 420–423, doi:10.1038/nphys583.
- Latham, T. L., P. Kumar, A. Nenes, J. Dufek, I. N. Sokolik, M. Trail, and A. Russell (2011), Hygroscopic properties of volcanic ash, *Geophys. Res. Lett.*, *38*, L11802, doi:10.1029/2011GL047298.
- Le Guern, F., A. Bernard, and R. M. Chevrier (1980), Soufriere of Guadeloupe 1976–1977 eruption—Mass and energy transfer and volcanic health hazards, *Bull. Volcanol.*, *43*, 577–593, doi:10.1007/BF02597694.
- Lewis, K. W., O. Aharonson, J. P. Grotzinger, S. W. Squyres, J. F. Bell III, L. S. Crumpler, and M. E. Schmidt (2008), Structure and stratigraphy of Home Plate from the Spirit Mars Exploration Rover, *J. Geophys. Res.*, *113*, E12S36, doi:10.1029/2007JE003025.
- Liu, C.-H., et al. (1995), Force fluctuation in bead packs, *Science*, *269*, 513–515, doi:10.1126/science.269.5223.513.
- Lorenz, V. (1973), On the formation of maars, *Bull. Volcanol.*, *37*, 183–204, doi:10.1007/BF02597130.
- Lorenz, V. (2007), Syn- and post-eruptive hazards of maar-diatreme volcanoes, *J. Volcanol. Geotherm. Res.*, *159*, 285–312, doi:10.1016/j.jvolgeores.2006.02.015.
- Mastin, L. G. (1991), The roles of magma and groundwater in the phreatic eruptions at Inyon craters, Long Valley caldera, California, *Bull. Volcanol.*, *53*, 579–596, doi:10.1007/BF00493687.
- Newhall, K. A., and D. J. Durian (2003), Projectile-shape dependence of impact craters in loose granular media, *Phys. Rev. Lett.*, *68*, 060301, doi:10.1103/PhysRevE.68.060301.
- Nishida, M., M. Okumura, and K. Tanaka (2010), Effects of density ratio and diameter ratio on critical incident angles of projectiles impacting granular media, *Granul. Matter*, *12*, 337–344, doi:10.1007/s10035-010-0186-7.
- Rice, M. S., A. E. Batista, J. F. Bell, and W. A. Watters (2010), Searching for “Home Plates” near Gusev Crater, Mars, Abstract P11B-1338 presented at 2010 Fall Meeting, AGU, San Francisco, Calif., 13–17 Dec.
- Richardson, M. I., and M. A. Mishna (2005), The long-term evolution of transient liquid water on Mars, *J. Geophys. Res.*, *110*, E03003, doi:10.1029/2004JE002367.
- Royer, J. R., B. Conyers, E. I. Corwin, P. J. Eng, and H. M. Jaeger (2011), The roles of interstitial gas in determining the impact response of granular beds, *Europhys. Lett.*, *93*, 28008, doi:10.1209/0295-5075/93/28008.
- Schmidt, M. E., et al. (2008), Hydrothermal origin of halogens at Home Plate, Gusev Crater, *J. Geophys. Res.*, *113*, E06S12, doi:10.1029/2007JE003027.
- Schmincke, H.-U. (2004), *Volcanism*, Springer, Berlin, doi:10.1007/978-3-642-18952-4.
- Self, S., J. Kienle, and J.-P. Huot (1980), Ukinrek Maars, Alaska, II. Deposits and formation of the 1977 craters, *J. Volcanol. Geotherm. Res.*, *7*, 39–65, doi:10.1016/0377-0273(80)90019-0.
- Sequin, A., Y. Bertho, and P. Gondret (2008), Influence of confinement on granular penetration by impact, *Phys. Rev. E*, *78*, 01030.
- Sklar, L. S., and W. E. Dietrich (2004), A mechanistic model for river incision into bedrock by saltating bed load, *Water Resour. Res.*, *40*, W06301, doi:10.1029/2003WR002496.
- Sottili, G., D. M. Palladino, M. Gaeta, and M. Masotta (2011), Origins and energetics of maar volcanoes: Examples from the ultrapotassic Sabatini volcanic district (Roman province, central Italy), *Bull. Volcanol.*, doi:10.1007/s00445-011-0506-8, in press.
- Squyres, S. W., et al. (2007), Pyroclastic activity at Home Plate in Gusev crater, *Science*, *306*, 1709–1714.
- Uehara, J. S., M. A. Ambroso, R. P. Ojha, and D. J. Durian (2003), Low-speed impact craters in loose granular media, *Phys. Rev. Lett.*, *90*, 194301, doi:10.1103/PhysRevLett.90.194301.
- Valentine, G. A., N. L. Shufelt, and A. M. Hintz (2011), Models of maar volcanoes, Lunar crater (Nevada, USA), *Bull. Volcanol.*, *73*, 753–765, doi:10.1007/s00445-011-0451-6.
- Wilson, L., and J. W. Head (2007), Explosive volcanic eruptions on Mars: Tephra and accretionary lapilli formation, dispersal, and recognition in the geologic record, *J. Volcanol. Geotherm. Res.*, *163*, 83–97, doi:10.1016/j.jvolgeores.2007.03.007.

J. Dufek, Earth and Atmospheric Sciences, Georgia Institute of Technology, Atlanta, GA 30332, USA.

E. S. Kite, M. Manga, and A. Patel, Department of Earth and Planetary Science and Center for Integrative Planetary Science, University of California, 307 McCone Hall, Berkeley, CA 94720, USA. (manga@seismo.berkeley.edu)